

## Phase and its morphologies of Ti-45%Al alloy directionally solidified at different growth rates<sup>①</sup>

LIU Chang(刘畅), SU Yan-qing(苏彦庆), BI Wei-sheng(毕维生),  
GUO Jing-Jie(郭景杰), JIA Jun(贾均), FU Heng-zhi(傅恒志)  
(School of Materials Science and Engineering, Harbin Institute of Technology,  
Harbin 150001, China)

**Abstract:** The microstructures of Ti-45%Al (molar fraction) alloy directionally solidified at different growth rates in alumina tube by electromagnetic heating zone melting were studied. The measured temperature gradient of the system is about  $10^4$  K/m. The microstructures show that the primary solidified phase is  $\beta$  phase at different growth rates. The growth at low rates from  $1.94 \times 10^{-6}$  m/s to  $4.16 \times 10^{-6}$  m/s results in a transient solid/liquid interface structure from planar to shallow cellular. This transient rate is larger than the theoretical value of  $v_c = 6.94 \times 10^{-7}$  m/s. Compared with  $v_t = v_c/k = 1.01 \times 10^{-6}$  m/s, the cellular-dendritic transient rate of experiment is observed in the range of  $1.67 \times 10^{-5}$  -  $2.50 \times 10^{-5}$  m/s. The primary arm spacing decreases with increasing growth rate.

**Key words:** Ti-45Al alloy; directional solidification; growth rate; interface structure

**CLC number:** TG 132.32

**Document code:** A

### 1 INTRODUCTION

In recent years, gamma TiAl based alloys have been extensively studied as potential structural materials in the aerospace, automotive and industrial applications because of their high specific strength at high temperature<sup>[1-3]</sup>. Due to the intrinsic anisotropy of lamellar microstructure of TiAl based alloys, Yamaguchi et al<sup>[2, 3]</sup> proposed that the mechanical properties of TiAl alloy under uniaxial loading could be improved with directional solidification techniques to align the lamellar orientation. Some success has been achieved in obtaining a microstructure that consists of columnar grains with each grain rotating around its longitudinal axis.

Despite that phase and morphology selection of peritectic alloys plays an important role on microstructure evolution<sup>[5]</sup>, little attention has been paid to the field of phase selection in TiAl alloys as a peritectic system during solidification. Some researchers have studied the phase and morphology selection relationship of many other peritectic alloys<sup>[6-9]</sup>. Kurz et al<sup>[6, 7]</sup> developed the criterion of the highest interface temperature that has been commonly used to predict phase and its morphologies. Hunziker et al<sup>[9]</sup> proposed a microstructure selection map for Fe-Ni peritectic systems giving the expected phase and its morphologies as a function of alloy composition and  $G/V$  ratio. They also

considered the effect of nucleation undercooling on the phase selection in Fe-Ni system.

The purpose of this paper is to study the effect of low growth rate on the phase and its morphologies of Ti-45%Al (molar fraction) alloy. With experimental measurement of temperature history of a given point of the TiAl sample during the direction solidification (DS) process, the temperature gradients of liquid were determined. That was necessary to apply the theoretical model to predict phase selection. Compared with the theoretical calculation results, the microstructures at different growth rates were analyzed. Based on the solid/liquid interface morphologies, the critical growth rates for the interface structure variation were determined.

### 2 EXPERIMENTAL

Ti-45%Al (molar fraction) alloy specimen with a diameter of 7 mm and length of 100 mm were inserted into a 99.9%  $Al_2O_3$  tube with inner diameter of 7.2 mm and outer diameter of 8.0 mm. Directional solidification (DS) was performed under an argon atmosphere with an induction heating zone melting apparatus. The apparatus was specially designed to be able to quench specimens during the DS process. DS experiments were carried out at withdrawing rates of  $1.94 \times 10^{-6}$  m/s,  $4.16 \times 10^{-6}$  m/s,  $8.33 \times 10^{-6}$  m/s,  $1.67 \times 10^{-5}$  m/s and

① **Foundation item:** Projects(50271020; 50395102) supported by the National Natural Science Foundation of China

**Received date:** 2004 - 12 - 05; **Accepted date:** 2005 - 01 - 18

**Correspondence:** LIU Chang, PhD Candidate; Tel: + 86-451-86418415; E-mail: suyq@hit.edu.cn

$2.50 \times 10^{-5}$  m/s respectively. After a given growing length, the sample contained in an alumina tube was quenched into a Ga-In liquid alloy pool. Thereby the structure of the solid/liquid interface was preserved. These samples were sectioned longitudinally, polished, and etched in a solution of 100 mL distilled water + 15 mL HF + 10 mL HNO<sub>3</sub>. The microstructures were investigated by optical microscopy (OM).

For a DS process, temperature gradient is very important. So we measured the temperature gradient of the applied DS apparatus firstly. In the TiAl sample a hole was cut with 2.6 mm in diameter. Then a B-type thermocouple was inserted into the hole. Before this stage, the thermocouple tip was enclosed in an alumina protective tube with outer diameter of 2.5 mm. The original position of the thermocouple tip was 20 mm above the induction coil. When the center part of the sample surrounded by the coils got a steady temperature, the sample was drawn into the cooling bath at a given rate. The temperature information was recorded automatically.

### 3 RESULTS

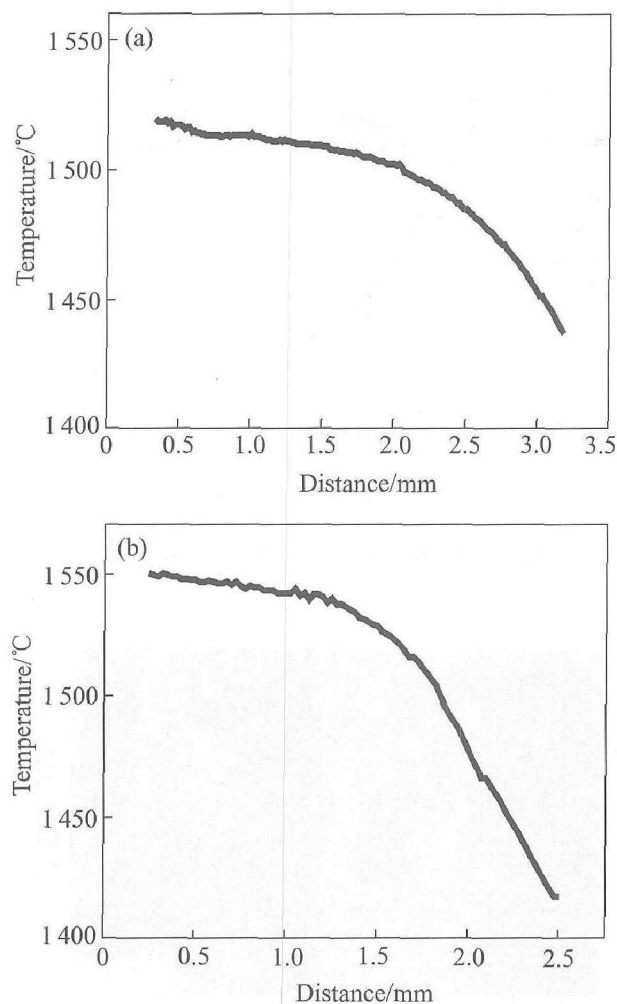
#### 3.1 Temperature gradient

Fig. 1 shows the temperature history of the measured point in the Ti-45% Al alloy during DS process at the growth rates of  $1.67 \times 10^{-5}$  m/s and  $2.50 \times 10^{-5}$  m/s. In Fig. 1 only the temperature range around the interface was plotted. From Fig. 1, the temperature gradient of liquid ( $G_L$ ) is about  $10 \times 10^3 - 13 \times 10^3$  K/m. The temperature gradient of liquid is  $(10 \pm 3) \times 10^3$  K/m at different growth rates. Hence, the temperature gradient of liquid is taken as  $10^4$  K/m during the theoretical analysis.

#### 3.2 DS microstructures and solid/liquid interface morphologies

The microstructures of these samples at different growth rates ( $1.94 \times 10^{-6}$  m/s,  $4.16 \times 10^{-6}$  m/s,  $8.33 \times 10^{-6}$  m/s,  $1.67 \times 10^{-5}$  m/s and  $2.50 \times 10^{-5}$  m/s) were observed respectively. As shown in Fig. 2, the samples at different growth rates exhibit typical DS columnar grains aligned along the growth direction. As shown in Fig. 3, when the growth rate is less than  $2.50 \times 10^{-5}$  m/s, the columnar grain thickness decreases with increasing growth rate. The columnar grains contain regular well-aligned  $\alpha/\gamma$  lamellar. The lamellar boundaries in the columnar grains of these samples incline at angles between  $0^\circ$  and  $45^\circ$ , as illustrated in Fig. 4.

Fig. 5 shows the solid/liquid interface morphologies these samples at different growth rates. A planar interface microstructure is formed at the



**Fig. 1** Temperature history of measured point in Ti-45% Al alloy at different growth rates  
(a)  $v = 1.67 \times 10^{-5}$  m/s; (b)  $v = 2.50 \times 10^{-5}$  m/s

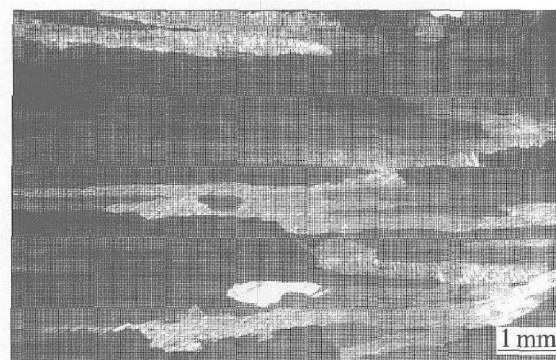


**Fig. 2** Typical columnar grains of Ti-45% Al grown at  $1.67 \times 10^{-5}$  m/s

growth rate of  $1.94 \times 10^{-6}$  m/s, as shown in Fig. 5 (a). Shallow cell interface is formed when the growth rate is  $4.16 \times 10^{-6}$  m/s, as shown in Fig. 5 (b). When the growth rate increases to  $1.67 \times 10^{-5}$  m/s, some cells show a tendency to translate to secondary dendrite arms and a transient structure composed of cells and dendrites is observed as shown in Fig. 5(c). When the growth rate increases to  $2.50 \times 10^{-5}$  m/s, the solid phase grows as dendrite, as shown in Fig. 5(d).

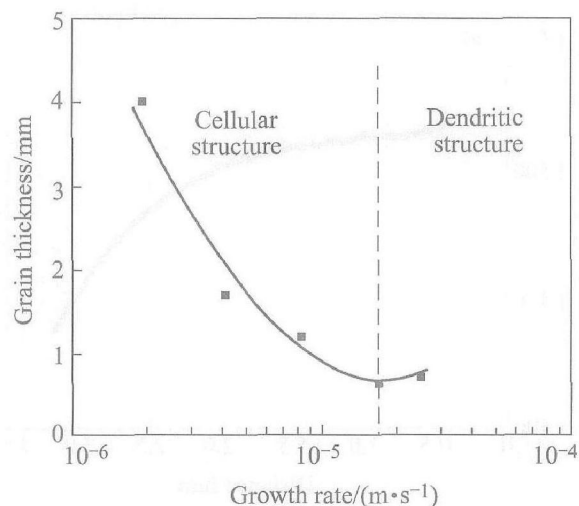


**Fig. 3** Dependence of columnar grain thickness on growth rate

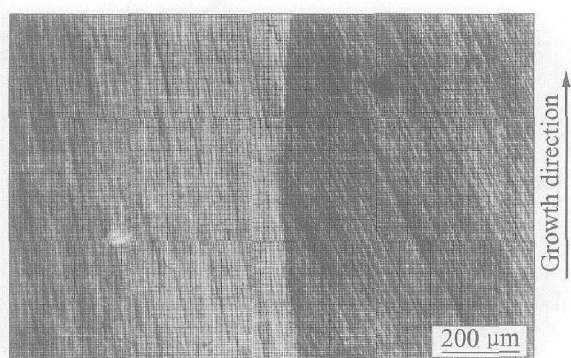


**Fig. 4** Lamellar morphology of Ti-45% Al alloy grown at  $4.16 \times 10^{-6}$  m/s

#### 4 DISCUSSION

The lamellar boundary orientations in the columnar grains of this alloy incline at angles between  $0^\circ$  and  $45^\circ$  with growth direction. According to the solid transformation procedure of  $\beta$  and  $\alpha$  to  $\alpha/\gamma$  lamellar<sup>[3,10,11]</sup>, as shown in Fig. 6, we can come to a conclusion that the primary phase during the DS process is the stable phase in Ti-45% Al alloy, namely  $\beta$  phase.

Taking the nucleation and compositional undercooling criterion<sup>[9]</sup>, the phase and morphology selection relationship of Ti-Al alloys is predicted, as shown in Fig. 7. With the increase of nucleation undercooling, the composition range of two-phase band structures decreases. That is to say, the composition range of growth zone of  $\beta$  phase (plane front and cells/dendrites) increases. If both  $\alpha$  and  $\beta$  phases nucleate without undercooling, Ti-45% Al alloy will solidify as band structure of alternative  $\alpha$  and  $\beta$  phases with planar interface. However, the experimental results show that Ti-45% Al alloy solidifies with only  $\beta$  phase and its morphologies varies with growth rate. These results are in agreement with the theoretical results as shown in Fig. 7 (b). Here, we assume the nucleation undercooling of two phases are all 2 K.

The experimental results show that the alloy solidifies with planar interface when the growth rate is  $1.94 \times 10^{-6}$  m/s. When the growth rate

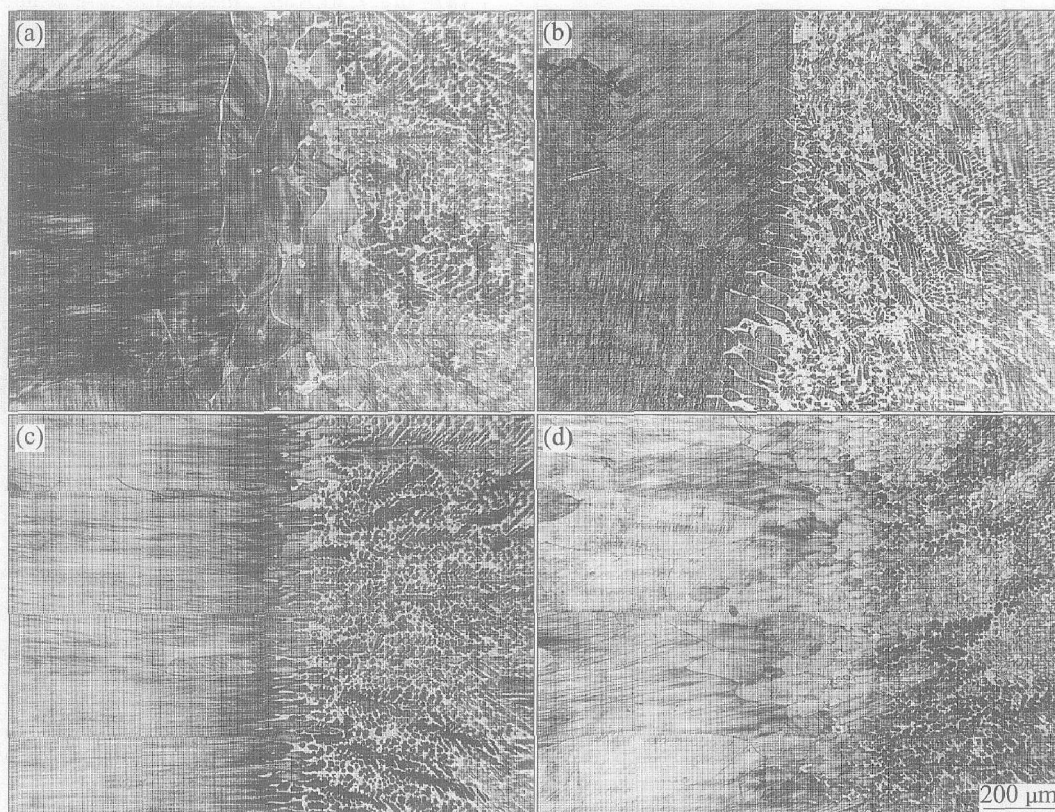


**Fig. 5** Quenched interface morphologies of Ti-45% Al alloy at different growth rates  
(a)  $v = 1.94 \times 10^{-6}$  m/s; (b)  $v = 4.16 \times 10^{-6}$  m/s; (c)  $v = 1.67 \times 10^{-5}$  m/s; (d)  $v = 2.50 \times 10^{-5}$  m/s

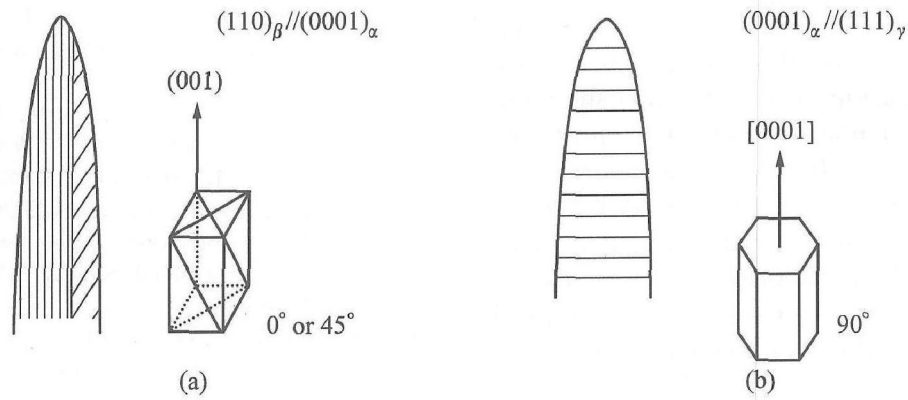


**Fig. 6** Lamellar orientations in  $\beta$  phase(a) and  $\alpha$  phase(b)

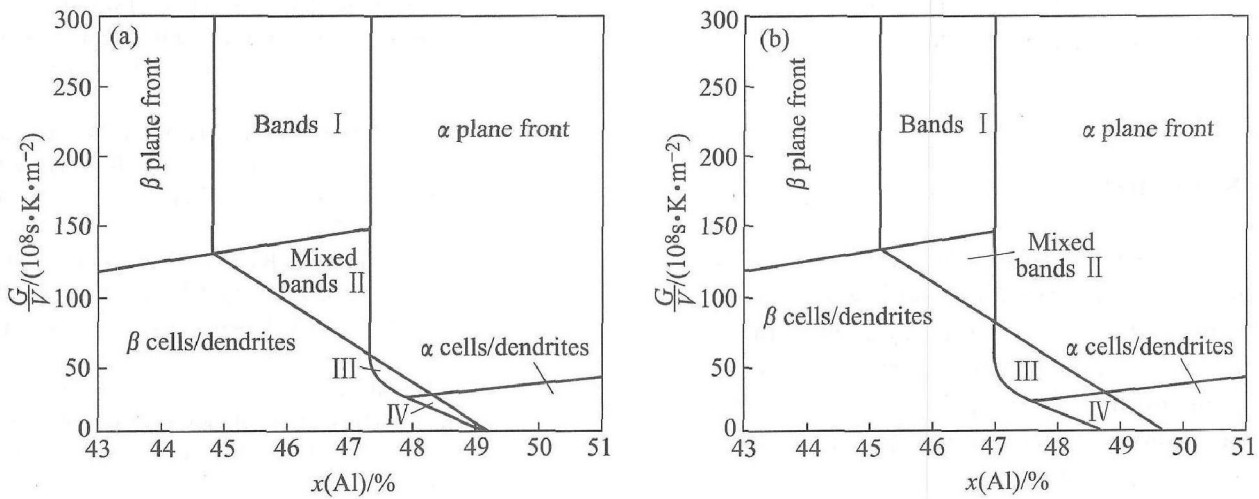


**Fig. 7** Phase and morphology selection relationship of Ti-Al system determined by nucleation and constitutional undercooling criterion

(a) —No nucleation undercooling; (b) —Nucleation undercooling of 2 K

increases to  $4.16 \times 10^{-6}$  m/s, the alloy solidifies with cellular interface. Hence, there is a transient rate of planar to cell/ dendrite between  $1.94 \times 10^{-6}$  m/s and  $4.16 \times 10^{-6}$  m/s. Based on interface response function (IRF) <sup>[12-14]</sup>, the forming sequences of  $\beta$  phase and its morphologies during the peritectic solidification processes of Ti-45Al are calculated ( $G_L = 10^4$  K/m), as shown in Fig. 8. The critical growth rate from planar to cell/ dendrite is  $v_c$ . The criterion for the stability of the planar solid/ liquid interface for TiAl alloys where  $\beta$  is primary solidification phase can be simplified as <sup>[15]</sup>

$$v_c = G_L D_L / \Delta T_0 \quad (1)$$

where  $G_L$  is the liquid temperature gradient at the solid/ liquid interface,  $\Delta T_0$  is the solidification intervals of the alloy (it comes from the phase diagram) and  $D_L$  is the diffusion coefficient in the liquid. The transition of planar interface to cellular should be theoretically observed at a critical growth rate of  $v_c = 6.92 \times 10^{-7}$  m/s, which is smaller than the experimental value. One reason for this may be the non-equilibrium freezing, which can minimize  $\Delta T_0$ .

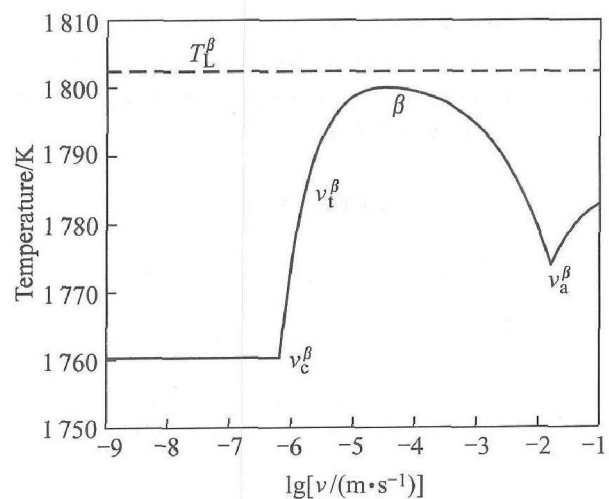


**Fig. 8** Interface response function(IRF) of  $\beta$  phase in Ti-45% Al alloy

The growth at low rates from  $1.94 \times 10^{-6}$  m/s to  $4.16 \times 10^{-6}$  m/s results in a transient structure from  $\beta$  phase planar solid/ liquid interface to shallow cellular interface. The growth at low rates from



$1.67 \times 10^{-5}$  m/s to  $2.50 \times 10^{-5}$  m/s results in the formation of  $\beta$  phase with a cellular-dendritic transient structure. When the growth rate is less than cellular dendrite transient rate, the cellular spacing decreases with increasing growth rate, as shown in Fig. 3. The experimentally observed evolution of primary cellular and dendritic spacing in the studied alloy has the same trend with the model of Kurz and Fisher<sup>[16]</sup>. It predicts a minimum in cellular spacing near the cellular-dendritic transition that is expected to occur at the transition growth rate of  $v_t = v_c/k$ , where  $k$  is the solute distribution coefficient. According to the experimental results,  $v_t$  is not equal to  $v_c/k$ , and  $v_t$  may be in the range of  $v_c/k^4$  to  $v_c/k^6$ . Kurz's model is developed for the dilution solution whose  $k$  is pretty small. However, the  $k$  value of TiAl alloy is very large. So the model should be modified to this form:

$$v_t = v_c/k^n \quad (n \geq 1) \\ (n = 1 \text{ for dilution solution}) \quad (2)$$

## 5 CONCLUSIONS

The microstructures of Ti-45% Al (molar fraction) alloy directionally solidified in alumina moulds by induction heating zone melting were studied. At a constant temperature gradient of  $10^4$  K/m in the liquid, the primary phase solidified from the liquid is  $\beta$  phase when growth rate varies in a large range from  $1.94 \times 10^{-6}$  m/s to  $2.50 \times 10^{-5}$  m/s. At lower growth rates from  $1.94 \times 10^{-6}$  m/s to  $4.16 \times 10^{-6}$  m/s, the interface structure changes from planar to shallow cellular. Cellular-dendritic transient structure is observed at the growth rates from  $1.67 \times 10^{-5}$  m/s to  $2.50 \times 10^{-5}$  m/s. When the growth rate is less than  $2.50 \times 10^{-5}$  m/s, the microstructure is composed of only  $\beta$  cellular grains and the cellular spacing decreases with increasing growth rate.

## REFERENCES

- [1] Dimiduk D M. Gamma titanium aluminide alloys—an assessment within the competition of aerospace structural materials [J]. Materials Science and Engineering, 1999, 263A: 281–288.
- [2] Kim S E, Lee Y T, Oh M H, et al. Directional solidification of TiAl-Si alloys using a polycrystalline seed [J]. Intermetallics, 2000, 8: 399–405.
- [3] Yamaguchi M, Johnson D R, Lee H N, et al. Directional solidification of TiAl alloys [J]. Intermetallics, 2000, 8: 511–517.
- [4] Lapin J, Ondrus L, Nazmy M. Directional solidification of intermetallic Ti-46Al-2W-0.5Si alloy in alumina moulds [J]. Intermetallics, 2002, 10: 1019–1031.
- [5] FU Heng-zhi, SU Yan-qing, GUO Jing-jie, et al. The solidification behavior of high temperature intermetallics [J]. Acta Metall Sinica, 2002, 38: 1127–1132. (in Chinese)
- [6] Kerr H W, Kurz W. Solidification of peritectic alloys [J]. International Materials Reviews, 1996, 41(4): 129–164.
- [7] Trivedi R. Theory of layered-structure formation in peritectic systems [J]. Metall Trans A, 1995, 26A: 1583–1590.
- [8] Lo T S, Dobler S, Plapp M, et al. Two-phase microstructure selection in peritectic solidification: from island banding to coupled growth [J]. Acta Mater, 2003, 51: 599–611.
- [9] Hunziker O, Vandyoussefi M, Kurz W. Phase and microstructure selection in peritectic alloys close to the limit of constitution undercooling [J]. Acta Mater, 1998, 46: 6325–6336.
- [10] Kishida K, Johnson D R, Masuda Y, et al. Deformation and fracture of PST crystals and directionally solidified ingots of TiAl-based alloys [J]. Intermetallics, 1998, 6: 679–683.
- [11] Inui H, Oh M H, Nakamura, et al. Room temperature tensile deformation of polysynthetically twinned (PST) crystals of TiAl [J]. Acta Mater, 1992, 40: 3095–3104.
- [12] Vandyoussefi M, Kerr H W, Kurz W. Directional solidification and  $\gamma/\gamma'$  solid state transformation in Fe-3% Ni alloys [J]. Acta Mater, 1997, 45: 4093–4105.
- [13] SU Yan-qing, LIU Chang, LI Xir-zhong, et al. Phase selection during directional peritectic solidification of Ti-Al binary system [J]. Intermetallics, 2005, 3–4: 267–274.
- [14] Umeda T, Ckane T, Kurz W. Phase selection during solidification of peritectic alloys [J]. Acta Mater, 1996, 44: 4209–4216.
- [15] Trivedi R, Kurz W. Modeling of solidification microstructure in concentrated solutions and intermetallic systems [J]. Metall Trans A, 1990, 21A: 1311–1318.
- [16] Kurz W, Fisher D J. Dendrite growth at the limit of stability: tip radius and spacing [J]. Acta Mater, 1981, 29: 11–20.

(Edited by YANG Bing)